Performance Analysis of Inter-Cell Interference Coordination in mm-Wave Cellular Networks

Haichao Wei, Na Deng, *Member, IEEE*, and Martin Haenggi, *Fellow, IEEE*

***Abstract*—In millimeter-wave (mm-wave) cellular networks, directional antenna arrays are typically adopted to mitigate the severe propagation loss. However, the interference caused by such highly directional beams may, in turn, result in a significant number of transmission failures, especially for dense networks. To tackle this problem, we propose two inter-cell interference coordination (ICIC) schemes in mm-wave bands: one is merely based on the path loss incorporating the blockage effect (PL-ICIC); the other considers both path loss and directivity gain (PG-ICIC). To fully investigate both schemes, we first derive an exact expression for the success probability (reliability) of the typical (served) user. We further provide an asymptotic analysis for the success probability and propose an effective approximation based on the asymptotic signal-to-interference ratio (SIR) gain relative to no ICIC. Secondly, to incorporate the cost of ICIC schemes, we derive the approximate normalized throughput taking into account that some users cannot be served due to limited resources. Numerical results show that the two proposed schemes provide significant reliability improvements in the low-SIR regime, and the higher the number of antennas, the wider the SIR range for which there is an improvement. In addition, compared with PL-ICIC, PG-ICIC balances the available resources among all users well.**

***Index Terms*—Millimeter-wave communication, inter-cell interference coordination, success probability, normalized throughput, stochastic geometry.**

I. Introduction

A. Motivation

Millimeter wave (mm-wave) networks, operating at frequencies between 30 and 300 GHz, have attracted considerable attention from both academia and industry due to the wide available bandwidth and the potential to offer high data rates [2, 3]. Compared with conventional microwave communications, mm-wave communications have new characteristics, making the deployment and operation of mm-wave cellular networks more challenging. Firstly, because of the higher frequencies, mm-wave signals are susceptible to the surrounding environments such as oxygen molecules and water vapor, which leads to significant path loss [4]. To address this issue, beamforming techniques are adopted to achieve substantial array gains and compensate the high propagation loss with large-scale antenna arrays (made possible due to the small wavelengths of the mm-wave band). Secondly, due to the poor diffraction, mm-wave signals are more vulnerable to blockage by most solid materials, which limits the coverage of mm-wave cellular networks. To overcome this limitation, mm-wave networks are envisioned to be densely deployed to shorten the serving distance to users and, in turn, achieve acceptable coverage and rate. However, as shown in [5, 6], increasing the density of base stations (BSs) beyond a certain point leads to performance degradation, and the network tends to be interference-limited, i.e., the main obstacle for successful transmission is the high level of interference. Furthermore, an interfering node might cause fatal interference if its highly directional beam points to the desired receiver, which deteriorates the quality of user experience. Hence, it is crucial to devise and study interference management techniques to avoid the adverse impact from the severe inter-cell interference in dense mm-wave cellular networks. This is challenging since the salient properties of mm-wave communication, such as the blockage effect and large antenna arrays, yield more complicated interference environments and thus complicate the design of efficient interference coordination schemes [7].

B. Related Work

An efficient approach to combat inter-cell interference in the downlink is to enable coordination between multiple BSs. The research of the coordination techniques focuses on the design of resource allocation schemes for performance optimization. In [8], the beamforming design and BS association policy are jointly optimized to maximize the long-term throughput with fairness guarantees. In [9], a coordinated frequency resource block allocation problem is formulated to maximize the minimum rate of the users, and a greedy scheme is adopted to solve this NP-hard integer programming problem. The authors in [10] jointly investigate the beam selection and transmit power allocation on the sub-carrier level to maximize the system sum rate. The above joint optimization problems usually require iterative algorithms to obtain the optimal (or sub-optimal) solutions, and the computational complexity increases with the number of optimization variables, which, in turn, depends on the number of the coordinated BSs, resource blocks, and the antenna array sizes. This complexity imposes restrictions on the practical implementation.

To cope with the complexity issue, deep learning-based approaches are employed to simplify the optimization procedure. For instance, a deep neural network (DNN) is adopted to approximate a conventional beam management and interference

Haichao Wei is with School of Information Science and Technology, Dalian Maritime University, Dalian 116026, China (e-mail: weihaichao@dlmu.edu.cn). Na Deng is with the School of Information and Communication Engineering, Dalian University of Technology, Dalian, 116024, China (e-mail: dengna@dlut.edu.cn). Martin Haenggi is with the Dept. of Electrical Engineering, University of Notre Dame, Notre Dame 46556, USA (e-mail: mhaenggi@nd.edu). (Corresponding author: Na Deng.)

Part of this paper has been published at the IEEE Global Communications Conference in 2019 [1]. This work has been supported by the National Natural Science Foundation of China under Grant 61701071, by the Fundamental Research Funds for the Central Universities DUT21JC04 and 3132019348, and by the US National Science Foundation through grant 2007498.

coordination algorithm in [11], which reduces the computation time of the outputs once the DNN is trained. However, the training process still consumes a host of computation and time resources. In [12], the authors propose a framework based on multi-armed bandits to learn the interference characteristics and then derive an optimal policy, where the resource allocation does not need to estimate current channel state information and thus the algorithm design is simplified. However, these works merely focus on the algorithmic design without considering the irregularity and variability of the node configurations in real networks, and the interference from the non-coordinated BSs are neglected. This motivates a stochastic geometry-based research approach to characterize the performance gain of interference coordination, where various point process models accurately capture different spatial characteristics of network nodes and the impact of the interference is fully considered.

As a powerful mathematical tool, stochastic geometry has recently been extensively used to model and analyze mm-wave networks for capturing the topological randomness in the network geometry while leading to a tractable analysis [13–16]. The BS coordination techniques, such as dynamic BS selection [17] and joint transmission [18, 19] have also been investigated using stochastic models for mm-wave networks. Both coordination schemes enhance system performance and end-user service quality through reducing the interference and improving the desired signal strength, but they require that the data for users be shared among the BSs participating in the coordinated transmission. This implies severe overheads of exchanging the signaling messages and user data through the inter-BS links (e.g., the X2 interface described in [20]) and hence degrades the system performance. Another promising BS coordination technique, termed inter-cell interference coordination (ICIC), does not require data sharing. The basic principle is to avoid strong interference from neighboring BSs, thereby improving the signal-to-interference ratio (SIR). Through muting certain time-frequency resource blocks (RBs) of adjacent cells, ICIC has been investigated in microwave networks [21–23], but the results do not apply in mm-wave networks.

Since the mm-wave spectrum has several unique features such as high propagation loss, sensitivity to blockage and large antenna arrays, the situation is quite different when ICIC is implemented in the mm-wave band. Regarding the interference characteristics, a key difference is that whether an interferer is dominant or not is not merely based on the distances or small-scale fading but on the power gains of the interfering beams and their line-of-sight/non-line-of-sight (LOS/NLOS) propagation states. For instance, the directivity deviation with narrow beams and the NLOS propagation significantly decreases the interference level from a nearby BS while a distant BS might cause fatal interference with the LOS propagation or its beam pointing to the receiver. In this case, an effective ICIC scheme should be carefully designed to only coordinate those BSs that actually cause significant interference. In [24], the interference from coordinated BSs is mitigated via a multi-cell zero-forcing precoder, and the rate complementary cumulative distribution function (CCDF) is analyzed with stochastic geometry to characterize the performance gain. The difficulty lies in exchanging the real-time channel state information and finding the digital precoding vectors to satisfy the zero-forcing criterion. In contrast, this paper investigates the ICIC schemes that mute certain BSs incorporating the LOS/NLOS states and the directional array gain, where analog beamformers are adopted to simplify the mm-wave transceiver structure and serve as the baseline beamforming technique. Such a scheme, to our best knowledge, has not been studied in mm-wave cellular networks.

C. Contribution

In this paper, we investigate ICIC in mm-wave cellular networks considering the unique characteristics of mm-wave communications. Specifically, the contributions are:

- Two ICIC schemes are proposed to improve the quality of experience for users: one is to mute certain RBs at certain BSs merely based on the path loss incorporating the blockage effect (PL-ICIC); the other is to mute certain RBs at certain BSs jointly considering the path loss and the directional array gain (PG-ICIC).
- Using stochastic geometry, we analyze the success probability to reflect the reliability gain of the users. To simplify the performance evaluation, the asymptotic success probability is derived when the SIR threshold tends to 0 and ∞. Based on the asymptotic results, we further provide approximate expressions for the success probabilities of the two proposed ICIC schemes.
- By taking into account that the muted RBs no longer serve users, the normalized throughput, defined as the success probability divided by the number of muted RBs due to ICIC, is proposed to characterize the overall network performance. This metric fully captures the performance gain of the served users and the cost of ICIC. Due the intricate dependence between the success probability and the number of muted RBs, the actual normalized throughput is intractable, and thus we propose the *approximate normalized throughput* (ANT) and derive its analytical expression.
- Numerical results demonstrate that both ICIC schemes yield significant performance gains in terms of the success probability over no ICIC and the nearest-ICIC (merely muting the nearest interfering BS) in the low-SIR regime, and that PL-ICIC is always better than PG-ICIC. In terms of the normalized throughput, PL-ICIC is worse than PG-ICIC and no ICIC because the muting operation based on the path loss causes more RBs to be muted, while PG-ICIC achieves better overall performance than no ICIC and nearest-ICIC with suitable coordination parameter setting and balances the available resources among all users well.

D. Organization

The rest of the paper is organized as follows. Section II introduces the network model and the proposed two ICIC schemes. Section III covers the performance analysis in terms of the success probability and the normalized throughput.

Section IV presents numerical results that show how the system parameters affect the performance achieved by the ICIC schemes, and Section V offers the concluding remarks.

II. System Model

A. Network Model

We consider an mm-wave cellular network where a homogeneous Poisson point process (PPP) Φ with density λ is used to model the location of the base stations (BSs). We consider the pertinent properties of mm-wave communications including directional beamforming of antenna arrays and blockage effect of the propagation environment. Each BS is assumed to be equipped with a uniform linear array (ULA) with N antenna elements, and a LOS probability function is adopted to capture the blockage effect [25, 26]. Specifically, we assume that all BSs know the angle of departure (AoD) to their serving users and apply analog beamforming with perfect beam alignment to obtain the maximum power gain[1]. Letting $w_{\rm m}$ be the half-power beamwidth (HPBW), we consider a normalized flat-top antenna pattern, given by

$$G(\varphi) = \begin{cases} G_{\rm m} & \text{if } |\varphi| \leq \frac{w_{\rm m}}{2} \\ G_{\rm s} & \text{otherwise,} \end{cases} \tag{1}$$

where $\varphi = \frac{d_{\rm t}}{\varrho}\cos\phi$ is the cosine direction corresponding to the AoD ϕ of the transmit signal, which is termed the *spatial AoD*, with $d_{\rm t}$ and ϱ representing the antenna spacing and wavelength, respectively. $d_{\rm t} = \frac{\varrho}{2}$ is chosen to enhance the directionality of the beam and avoid grating lobes; φ is assumed to be uniformly distributed in $[-0.5, 0.5]$. It is known from [27] that the actual antenna pattern of the ULA is

$$G_{\rm act}(\varphi) = \frac{\sin^2(\pi N \varphi)}{N \sin^2(\pi\varphi)}, \tag{2}$$

and we have $G_{\rm m} = N$, $G_{\rm act}(\frac{w_{\rm m}}{2}) = \frac{N}{2}$ and $G_{\rm s} = \frac{1-w_{\rm m}G_{\rm m}}{1-w_{\rm m}}$.

In the LOS probability function, the LOS probability of the channel between two nodes with separation r is

$$p_{\rm L}(r) = \exp(-\beta r), \tag{3}$$

where $\beta > 0$ is the parameter to characterize the blockage effect and depends on the density and shape of blockages [25, 26], and the NLOS probability is denoted by $p_{\rm N}(r) = 1 - p_{\rm L}(r)$. The stationarity of the PPP lends itself to the analysis for the typical user located at the origin. From the perspective of the typical user, the BSs in Φ can be partitioned into two classes due to the blockage effect: The BSs with LOS propagation form a non-homogeneous PPP $\Phi_{\rm L}$, while $\Phi_{\rm N} = \Phi \setminus \Phi_{\rm L}$ denotes the BS set with NLOS propagation. Each x in Φ is assigned to $\Phi_{\rm L}$ with probability $p_{\rm L}(|x|)$ and to $\Phi_{\rm N}$ otherwise, independently for all x in Φ. The probability that $\Phi_{\rm L}$ is an empty set is $\mathbb{P}(\Phi_{\rm L} = \emptyset) = e^{-2\pi\lambda/\beta^2}$. We denote by $\alpha_{\rm L}$ and $\alpha_{\rm N}$ the path loss exponents for LOS and NLOS channels, respectively. Let $\ell(x) = |x|^{-\alpha_x}$ be the random path loss function from x to the origin, where $\alpha_x \in \{\alpha_{\rm L}, \alpha_{\rm N}\}$. Nakagami fading is adopted to model the small-scale fading. For $x \in \Phi_{\rm L}$, $\alpha_x = \alpha_{\rm L}$ and its power fading coefficient h_x follows a gamma distribution $\mathrm{Gamma}(M_{\rm L}, \frac{1}{M_{\rm L}})$, while for $x \in \Phi_{\rm N}$, $\alpha_x = \alpha_{\rm N}$ and h_x follows a gamma distribution $\mathrm{Gamma}(M_{\rm N}, \frac{1}{M_{\rm N}})$. Furthermore, all h_x are mutually independent and also independent of Φ.

B. Proposed ICIC Schemes

The typical user has a single antenna and is served by the BS with the smallest path loss, i.e., the serving BS x_0 is given by

$$x_0 = \arg\max\left\{x \in \Phi : |x|^{-\alpha_x}\right\}, \tag{4}$$

and the serving BS assigns one RB to the typical user for data transmission[2]. The serving BS is not always the nearest BS to the typical user. We consider an interference-limited mm-wave cellular network[3], and the transmit power of the BSs can be set to 1 without loss of generality. The SIR at the typical user is

$$\mathrm{SIR} = \frac{G_{\rm m} h_{x_0} |x_0|^{-\alpha_{x_0}}}{\sum_{x\in\Phi^!} G(\varphi_x) h_x \ell(x)}, \tag{5}$$

where $\Phi^! = \Phi \setminus \{x_0\}$ and $G(\varphi_x)$ follows from (1). As in [5], the spatial AoD φ_x from an interferer to the typical user is uniformly distributed in $[-0.5, 0.5]$. To combat the inter-cell interference, we consider two ICIC schemes as follows.

1) Path loss-based ICIC (PL-ICIC): The BSs in the coordinating set

$$\Omega_{\rm PL} = \left\{x \in \Phi^! : |x|^{-\alpha_x} > (1-\rho)|x_0|^{-\alpha_{x_0}}\right\} \tag{6}$$

are muting the RB assigned to the typical user, and $\rho \in [0, 1]$ is a parameter that characterizes the coordination level. $\rho = 0$ means no coordination ($\Omega_{\rm PL} = \emptyset$) while $\rho = 1$ is full coordination ($\Omega_{\rm PL} = \Phi^!$). In this case, whether a BS participates in the interference coordination depends on its path loss to the typical user, which is related to the blockage effect from interfering BSs to the typical user. The SIR at the typical user with PL-ICIC is

$$\mathrm{SIR}_{\rm PL} = \frac{G_{\rm m} h_{x_0} |x_0|^{-\alpha_{x_0}}}{\sum_{x\in\Phi^!\setminus\Omega_{\rm PL}} G(\varphi_x) h_x \ell(x)}. \tag{7}$$

When $\rho = 0$, no ICIC occurs, and $\mathrm{SIR}_{\rm PL}$ becomes (5).

2) Path loss and array gain-based ICIC (PG-ICIC): Jointly considering the blockage effect and the directional array gain, the BSs in the coordinating set

$$\Omega_{\rm PG} = \left\{x \in \Phi^! : G(\varphi_x)|x|^{-\alpha_x} > (1-\rho)G_{\rm m}|x_0|^{-\alpha_{x_0}}\right\} \tag{8}$$

are muting the RB assigned to the typical user. The SIR at the typical user with PG-ICIC is

$$\mathrm{SIR}_{\rm PG} = \frac{G_{\rm m} h_{x_0} |x_0|^{-\alpha_{x_0}}}{\sum_{x\in\Phi^!\setminus\Omega_{\rm PG}} G(\varphi_x) h_x \ell(x)}. \tag{9}$$

When $\rho = 0$, no ICIC occurs, and $\mathrm{SIR}_{\rm PG}$ also reverts to (5).

[1] Analog beamforming, as a baseline approach, provides a low-complexity and low-cost scheme for mm-wave communications with massive antenna arrays, and the perfect beam alignment assumption is to achieve the maximum antenna gain and facilitate the performance analysis.

[2] If multiple RBs are assigned to a user, the performance can be evaluated by considering the individual RBs and appropriate combining.

[3] If the network was purely noise-limited, there would be a push towards increasing the transmit power levels or BS densities, which would result in an increased throughput and make interference become the performance-limiting factor.

When the two ICIC schemes are implemented in practical systems, the serving BS sends the received signal strength measured by a target user, user location, and coordination level ρ to its neighboring BSs, and whether a neighboring BS needs to participate in the coordination is determined by comparing the path loss and array gain to the target user.

III. Performance Analysis

In this section, we first derive the association probabilities and the distributions of the serving distances to the LOS/NLOS BSs. Then we give the exact results on the success probability for the typical user and the normalized throughput for all users.

A. Association Probability and Link Distance

Lemma 1. *The probability that $x_0 \in \Phi_{\mathrm{L}}$ is*

$$A_{\mathrm{L}} = 2\pi\lambda \int_0^\infty r e^{-\beta r} \exp\Big(-2\pi\lambda\Big(\frac{r^{2\alpha_{\mathrm{L}}/\alpha_{\mathrm{N}}}}{2} + e^{-\beta r^{\alpha_{\mathrm{L}}/\alpha_{\mathrm{N}}}} \frac{1+\beta r^{\alpha_{\mathrm{L}}/\alpha_{\mathrm{N}}}}{\beta^2} - e^{-\beta r}\frac{1+\beta r}{\beta^2}\Big)\Big)\mathrm{d}r, \quad (10)$$

and the probability that $x_0 \in \Phi_{\mathrm{N}}$ is $A_{\mathrm{N}} = 1 - A_{\mathrm{L}}$.

Proof: Using the representation [28, Eqn. (18)] and following the Campbell-Mecke theorem [29, Thm. 8.2], the probability that the typical user is associated with a LOS BS, i.e., $x_0 \in \Phi_{\mathrm{L}}$, is expressed by

$$\begin{aligned} A_{\mathrm{L}} &= \mathbb{E}\sum_{x\in\Phi} p_{\mathrm{L}}(|x|) \prod_{y\in\Phi\setminus\{x\}} \mathbf{1}_{|x|^{-\alpha_{\mathrm{L}}} > |y|^{-\alpha_y}} \\ &= \lambda \int_{\mathbb{R}^2} \mathbb{E}\Big[\prod_{y\in\Phi\setminus\{x\}} \mathbf{1}_{|x|^{-\alpha_{\mathrm{L}}} > |y|^{-\alpha_y}}\Big] p_{\mathrm{L}}(|x|)\mathrm{d}x \\ &\overset{(a)}{=} \lambda \int_{\mathbb{R}^2} \mathbb{E}\Big[\prod_{y\in\Phi} \mathbf{1}_{|x|^{-\alpha_{\mathrm{L}}} > |y|^{-\alpha_y}}\Big] p_{\mathrm{L}}(|x|)\mathrm{d}x \\ &= 2\pi\lambda \int_0^\infty \exp\Big(-2\pi\lambda \int_0^\infty (1 - e^{-\beta t}\mathbf{1}_{r^{-\alpha_{\mathrm{L}}} > t^{-\alpha_{\mathrm{L}}}} \\ &\quad -(1-e^{-\beta t})\mathbf{1}_{r^{-\alpha_{\mathrm{L}}} > t^{-\alpha_{\mathrm{N}}}}) t\mathrm{d}t\Big) r e^{-\beta r}\mathrm{d}r \\ &= 2\pi\lambda \int_0^\infty \exp\Big(-2\pi\lambda\Big(\frac{r^{2\alpha_{\mathrm{L}}/\alpha_{\mathrm{N}}}}{2} - e^{-\beta r}\frac{1+\beta r}{\beta^2} \\ &\quad + e^{-\beta r^{\alpha_{\mathrm{L}}/\alpha_{\mathrm{N}}}} \frac{1+\beta r^{\alpha_{\mathrm{L}}/\alpha_{\mathrm{N}}}}{\beta^2}\Big)\Big) r e^{-\beta r}\mathrm{d}r. \end{aligned} \quad (11)$$

Since the typical user is served by either a LOS BS or a NLOS BS, we have $A_{\mathrm{N}} = 1 - A_{\mathrm{L}}$. ■

When $\alpha_{\mathrm{L}} = \alpha_{\mathrm{N}} = \alpha$, we have the simple expression of $A_{\mathrm{L}} = 1 - e^c\sqrt{\pi c}\,\mathrm{erfc}(\sqrt{c})$ with the help of [30, Eq. 3.326.3], where $c = \frac{\beta^2}{4\pi\lambda}$ in this case and $1/c$ is the mean number of points in a disk of radius $2/\beta$. Since both the desired signal strength and the muting operation of non-serving BSs depend on the distance between the typical user and its serving BS, the following lemma gives the distribution of this distance. Although previous works have given the results and the corresponding proofs [25, 26], we provide an alternative approach to obtain the distribution using the Campbell-Mecke theorem.

Lemma 2. *Given that the typical user is associated with a LOS/NLOS BS, the probability density function (PDF) of the distance $r_0 = |x_0|$ between the typical user and its serving BS is*

$$f_{r_0|x_0\in\Phi_k}(r) = f_k(r)/A_k, \quad k \in \{\mathrm{L}, \mathrm{N}\}, \quad (12)$$

where

$$\begin{aligned} f_{\mathrm{L}}(r) &= 2\pi\lambda r e^{-\beta r} \exp\Big(-2\pi\lambda\Big(\frac{r^{2\alpha_{\mathrm{L}}/\alpha_{\mathrm{N}}}}{2} \\ &\quad + e^{-\beta r^{\alpha_{\mathrm{L}}/\alpha_{\mathrm{N}}}} \frac{1+\beta r^{\alpha_{\mathrm{L}}/\alpha_{\mathrm{N}}}}{\beta^2} - e^{-\beta r}\frac{1+\beta r}{\beta^2}\Big)\Big), \\ f_{\mathrm{N}}(r) &= 2\pi\lambda r(1-e^{-\beta r}) \exp\Big(-2\pi\lambda\Big(\frac{r^2}{2} + e^{-\beta r}\frac{1+\beta r}{\beta^2} \\ &\quad - e^{-\beta r^{\alpha_{\mathrm{N}}/\alpha_{\mathrm{L}}}} \frac{1+\beta r^{\alpha_{\mathrm{N}}/\alpha_{\mathrm{L}}}}{\beta^2}\Big)\Big). \end{aligned} \quad (13)$$

Proof: Given that the typical user is associated with a LOS BS, the complementary cumulative distribution function (CCDF) of $|x_0|$ is given by

$$\begin{aligned} &\mathbb{P}(|x_0| > r \mid x_0 \in \Phi_{\mathrm{L}}) \\ &= \frac{\mathbb{P}(|x_0| > r, x_0 \in \Phi_{\mathrm{L}})}{A_{\mathrm{L}}} \\ &= \frac{1}{A_{\mathrm{L}}}\mathbb{E}\sum_{x\in\Phi} p_{\mathrm{L}}(|x|)\mathbf{1}_{|x|>r} \prod_{y\in\Phi\setminus\{x\}} \mathbf{1}_{|x|^{-\alpha_{\mathrm{L}}} > |y|^{-\alpha_y}} \\ &= \frac{2\pi\lambda}{A_{\mathrm{L}}} \int_r^\infty \exp\Big(-2\pi\lambda\Big(\frac{t^{2\alpha_{\mathrm{L}}/\alpha_{\mathrm{N}}}}{2} - e^{-\beta t}\frac{1+\beta t}{\beta^2} \\ &\quad + e^{-\beta t^{\alpha_{\mathrm{L}}/\alpha_{\mathrm{N}}}} \frac{1+\beta t^{\alpha_{\mathrm{L}}/\alpha_{\mathrm{N}}}}{\beta^2}\Big)\Big) t e^{-\beta t}\mathrm{d}t. \end{aligned} \quad (14)$$

Hence the conditional PDF of $|x_0|$ is obtained by deriving the first-order derivative of the CCDF w.r.t. r, given by

$$\begin{aligned} f_{r_0|x_0\in\Phi_{\mathrm{L}}}(r) &= \frac{2\pi\lambda}{A_{\mathrm{L}}} r e^{-\beta r} \exp\Big(-2\pi\lambda\Big(\frac{r^{2\alpha_{\mathrm{L}}/\alpha_{\mathrm{N}}}}{2} \\ &\quad + e^{-\beta r^{\alpha_{\mathrm{L}}/\alpha_{\mathrm{N}}}} \frac{1+\beta r^{\alpha_{\mathrm{L}}/\alpha_{\mathrm{N}}}}{\beta^2} - e^{-\beta r}\frac{1+\beta r}{\beta^2}\Big)\Big). \end{aligned} \quad (15)$$

Given that the typical user is associated with a NLOS BS, the conditional PDF of $|x_0|$ is similarly given by

$$\begin{aligned} f_{r_0|x_0\in\Phi_{\mathrm{N}}}(r) &= \frac{2\pi\lambda}{A_{\mathrm{N}}} r(1-e^{-\beta r}) \exp\Big(-2\pi\lambda\Big(\frac{r^2}{2} \\ &\quad + e^{-\beta r}\frac{1+\beta r}{\beta^2} - e^{-\beta r^{\alpha_{\mathrm{N}}/\alpha_{\mathrm{L}}}} \frac{1+\beta r^{\alpha_{\mathrm{N}}/\alpha_{\mathrm{L}}}}{\beta^2}\Big)\Big). \end{aligned} \quad (16)$$

■

B. Success Probability of the Typical Served User

The success probability is defined as the CCDF of the SIR, given by

$$P(\theta) = \mathbb{P}(\mathrm{SIR} > \theta), \quad (17)$$

where θ is target SIR threshold. The success probability can be thought of equivalently as the probability that the typical user achieves a target SIR θ or the fraction of users who achieve an SIR of θ in any time slot in any realization of the PPP. Since the desired signal link is either LOS or NLOS, the success probability is obtained by using the total probability law, expressed as

$$P(\theta) = P_{\mathrm{L}}(\theta) + P_{\mathrm{N}}(\theta), \tag{18}$$

where P_{L} and P_{N} are the joint probabilities that $\mathrm{SIR} > \theta$ and the desired link is LOS and NLOS, respectively. Our first result in this section is an exact expression of the success probability with the PL-ICIC scheme.

Theorem 1. *Let* $w_{\mathrm{s}} \triangleq 1 - w_{\mathrm{m}}$, $\bar{r}_{k,i} \triangleq (\frac{r^{\alpha_k}}{1-\rho})^{1/\alpha_i}$,

$$\eta_k(r,u) \triangleq -2\pi\lambda \sum_{j\in\{\mathrm{m,s}\}} \sum_{i\in\{\mathrm{L,N}\}} w_j \times \int_{\bar{r}_{k,i}}^{\infty} \Big(1 - \frac{1}{(1+\frac{uG_j y^{-\alpha_i}}{M_i})^{M_i}}\Big) p_i(y) y \mathrm{d}y, \tag{19}$$

$\mathcal{L}_k(r,u) = \exp(\eta_k(r,u))$, $\mathcal{L}_k^{(l)}(r,u)$ *denote the l-th derivative of $\mathcal{L}_k(r,u)$ w.r.t. u, and*

$$P_k(\theta) \triangleq \sum_{l=0}^{M_k-1} \int_0^{\infty} f_k(r) \frac{(-u)^l}{l!} \mathcal{L}_k^{(l)}(r,u)|_{u=\frac{\theta M_k}{G_{\mathrm{m}}} r^{\alpha_k}} \mathrm{d}r. \tag{20}$$

For the PL-ICIC scheme, the success probability of the typical user is given by

$$P_{\mathrm{PL}}(\theta) = \sum_{k\in\{\mathrm{L,N}\}} P_k(\theta), \tag{21}$$

where $\mathcal{L}_k^{(l)}(r,u)$ is given recursively by

$$\mathcal{L}_k^{(l)}(r,u) = \sum_{n=0}^{l-1} \binom{l-1}{n} \eta_k^{(l-n)}(r,u) \mathcal{L}_k^{(n)}(r,u), \tag{22}$$

and the n-th derivative of $\eta_k(r,u)$ w.r.t. u is

$$\eta_k^{(n)}(r,u) = 2\pi\lambda \sum_{j\in\{\mathrm{m,s}\}} \sum_{i\in\{\mathrm{L,N}\}} w_j \Big(-\frac{G_j}{M_i}\Big)^n \frac{\Gamma(M_i+n)}{\Gamma(M_i)} \times \int_{\bar{r}_{k,i}}^{\infty} \frac{p_i(y) y^{1-n\alpha_i}}{(1+\frac{uG_j y^{-\alpha_i}}{M_i})^{M_i+n}} \mathrm{d}y. \tag{23}$$

Proof: See Appendix A.

Next, we give an exact expression of the success probability for the typical user with the PG-ICIC scheme.

Theorem 2. *Let* $\tilde{r}_{k,i,j} \triangleq \max\big(1, (\frac{G_j}{(1-\rho)G_{\mathrm{m}}})^{1/\alpha_i}\big) r^{\alpha_k/\alpha_i}$,

$$\widetilde{\eta}_k(r,u) \triangleq -2\pi\lambda \sum_{j\in\{\mathrm{m,s}\}} \sum_{i\in\{\mathrm{L,N}\}} w_j \times \int_{\tilde{r}_{k,i,j}}^{\infty} \Big(1 - \frac{1}{(1+\frac{uG_j y^{-\alpha_i}}{M_i})^{M_i}}\Big) p_i(y) y \mathrm{d}y, \tag{24}$$

$\widetilde{\mathcal{L}}_k(r,u) = \exp(\widetilde{\eta}_k(r,u))$, $\widetilde{\mathcal{L}}_k^{(l)}(r,u)$ *denote the l-th derivative of $\widetilde{\mathcal{L}}_k(r,u)$ w.r.t. u and*

$$\widetilde{P}_k(\theta) \triangleq \sum_{l=0}^{M_k-1} \int_0^{\infty} f_k(r) \frac{(-u)^l}{l!} \widetilde{\mathcal{L}}_k^{(l)}(r,u)|_{u=\frac{\theta M_k}{G_{\mathrm{m}}} r^{\alpha_k}} \mathrm{d}r. \tag{25}$$

For the PG-ICIC scheme, the success probability of the typical user is given by

$$P_{\mathrm{PG}}(\theta) = \sum_{k\in\{\mathrm{L,N}\}} \widetilde{P}_k(\theta), \tag{26}$$

where $\widetilde{\mathcal{L}}_k^{(l)}(r,u)$ is given recursively similar to Theorem 1.

Proof: The proof is analogous to that of Theorem 1, with a modified spatial distribution of the interfering BSs according to the coordinating set Ω_{PG}. ■

Remark 1: Comparing Ω_{PL} and Ω_{PG}, we find that $\Omega_{\mathrm{PG}} \subseteq \Omega_{\mathrm{PL}}$ for fixed ρ. This is because any BS $x \in \Omega_{\mathrm{PG}}$ satisfies $G_{\mathrm{m}}\ell(x) \geq G(\varphi_x)\ell(x) > (1-\rho)G_{\mathrm{m}}\ell(x_0)$, and thus $x \in \Omega_{\mathrm{PL}}$. Hence the interference under the PG-ICIC scheme is no less than that under the PL-ICIC scheme. As a result, we have $P(\theta) \geq \widetilde{P}(\theta)$.

C. Asymptotic Analysis

The exact results in Thm. 1 and 2 have complex forms. They involve the computation of the derivatives of the Laplace transform of the interference and the evaluation of nested integrals. To simplify the performance evaluation, we provide asymptotic analyses[4] for $\theta \to 0$ and $\theta \to \infty$ to quantify the performance gain of the two proposed ICIC schemes in the low- and high-SIR regimes. For notational convenience, we define

$$\chi_{\mathrm{L}}(x,\beta,n) \triangleq \beta^{n\alpha_{\mathrm{L}}-2}\Gamma(2-n\alpha_{\mathrm{L}},\beta x)$$
$$\chi_{\mathrm{N}}(x,\beta,n) \triangleq \frac{x^{2-n\alpha_{\mathrm{N}}}}{n\alpha_{\mathrm{N}}-2} - \beta^{n\alpha_{\mathrm{N}}-2}\Gamma(2-n\alpha_{\mathrm{N}},\beta x). \tag{27}$$

Corollary 1. *For the PL-ICIC scheme,*

$$1 - P_{\mathrm{PL}}(\theta) \sim \sum_{k\in\{\mathrm{L,N}\}} \Psi_k(\rho)\theta^{M_k}, \quad \theta \to 0, \tag{28}$$

where

$$\Psi_k(\rho) = \frac{(-M_k)^{M_k}}{\Gamma(M_k+1)G_{\mathrm{m}}^{M_k}} \int_0^{\infty} f_k(r) r^{M_k\alpha_k} \mathcal{L}_k^{(M_k)}(r,u)|_{u=0} \mathrm{d}r, \tag{29}$$

and $\mathcal{L}_k^{(M_k)}(r,u)|_{u=0}$ can be calculated in a recursive manner using

$$\mathcal{L}_k^{(l)}(r,0) = \sum_{n=0}^{l-1} \binom{l-1}{n} \eta_k^{(l-n)}(r,0) \mathcal{L}_k^{(n)}(r,0), \tag{30}$$

where $\mathcal{L}_k(r,0) = 1$, $\eta_k(r,0) = 0$, and

$$\eta_k^{(n)}(r,0) = 2\pi\lambda \sum_{j\in\{\mathrm{m,s}\}} \sum_{i\in\{\mathrm{L,N}\}} w_j \Big(-\frac{G_j}{M_i}\Big)^n \times \frac{\Gamma(M_i+n)}{\Gamma(M_i)} \chi_i(\bar{r}_{k,i},\beta,n). \tag{31}$$

[4]For two functions $f(x)$ and $g(x)$, $f(x) \sim g(x)$, $x \to x_0$ means that $f(x)$ is asymptotically equivalent to $g(x)$, as $x \to x_0$, mathematically expressed by $\lim_{x\to x_0} f(x)/g(x) = 1$.

Proof: The success probability of the PL-ICIC scheme is

$$\begin{aligned}P_{\mathrm{PL}}(\theta) &= \sum_{k\in\{\mathrm{L,N}\}} A_k \mathbb{P}\Big(\frac{G_{\mathrm{m}} h_{x_0} r_0^{-\alpha_k}}{I} > \theta\Big)\\ &= \sum_{k\in\{\mathrm{L,N}\}} A_k \mathbb{E}\Big[\widetilde{\Gamma}\big(M_k, \tilde{\theta}_k r_0^{\alpha_k} I\big)\Big]\\ &= \sum_{k\in\{\mathrm{L,N}\}} A_k \Big(1-\mathbb{E}\Big[\widetilde{\gamma}\big(M_k, \tilde{\theta}_k r_0^{\alpha_k} I\big)\Big]\Big)\\ &= 1-\sum_{k\in\{\mathrm{L,N}\}} A_k \mathbb{E}\Big[\widetilde{\gamma}\big(M_k, \tilde{\theta}_k r_0^{\alpha_k} I\big)\Big], \end{aligned} \tag{32}$$

where $\tilde{\theta}_k = \frac{\theta M_k}{G_{\mathrm{m}}}$, and $\widetilde{\gamma}(x,y) = \gamma(x,y)/\Gamma(x)$ is the normalized lower incomplete gamma function. Hence we have

$$\begin{aligned}&1-P_{\mathrm{PL}}(\theta)\\ &\sim \sum_{k\in\{\mathrm{L,N}\}} \frac{A_k \tilde{\theta}_k^{M_k}}{\Gamma(M_k+1)} \mathbb{E}\big[r_0^{\alpha_k} I\big]^{M_k},\ \theta\to 0\\ &\sim \sum_{k\in\{\mathrm{L,N}\}} \frac{(-\tilde{\theta}_k)^{M_k}}{\Gamma(M_k+1)} \int_0^\infty f_k(r) r^{M_k\alpha_k} \mathcal{L}_k^{(M_k)}(r,u)|_{u=0}\,\mathrm{d}r,\ \theta\to 0,\end{aligned} \tag{33}$$

where $\mathbb{E}I^m = (-1)^m \mathcal{L}_k^{(m)}(r,u)|_{u=0}$. Through substituting $u=0$ into $\eta_k(r,u)$ and its derivatives, the final result is obtained. ■

Corollary 2. *For the PG-ICIC scheme,*

$$1-P_{\mathrm{PG}}(\theta) \sim \sum_{k\in\{\mathrm{L,N}\}} \widetilde{\Psi}_k(\rho)\theta^{M_k}, \quad \theta\to 0, \tag{34}$$

where

$$\widetilde{\Psi}_k(\rho) = \frac{(-M_k)^{M_k}}{\Gamma(M_k+1)G_{\mathrm{m}}^{M_k}} \int_0^\infty f_k(r) r^{M_k\alpha_k} \widetilde{\mathcal{L}}_k^{(M_k)}(r,u)|_{u=0}\mathrm{d}r, \tag{35}$$

and $\widetilde{\mathcal{L}}_k^{(M_k)}(r,u)|_{u=0}$ *can be calculated in a recursive manner using*

$$\widetilde{\mathcal{L}}_k^{(l)}(r,0) = \sum_{n=0}^{l-1} \binom{l-1}{n} \widetilde{\eta}_k^{(l-n)}(r,0) \widetilde{\mathcal{L}}_k^{(n)}(r,0), \tag{36}$$

where $\widetilde{\mathcal{L}}_k(r,0)=1$, $\widetilde{\eta}_k(r,0)=0$, *and*

$$\begin{aligned}\widetilde{\eta}_k^{(n)}(r,0) = 2\pi\lambda &\sum_{j\in\{\mathrm{m,s}\}} \sum_{i\in\{\mathrm{L,N}\}} w_j \Big(-\frac{G_j}{M_i}\Big)^n\\ &\times \frac{\Gamma(M_i+n)}{\Gamma(M_i)} \chi_i(\tilde{r}_{k,i,j}, \beta, n).\end{aligned} \tag{37}$$

Proof: The proof is analogous to that of Corollary 1. ■

Remark 2: Corollaries 1 and 2 show that the asymptotic behavior of the success probability has the same form for the proposed two schemes, where the two pre-constants $\Psi_k(\rho), k\in\{\mathrm{L,N}\}$ (or $\widetilde{\Psi}_k(\rho)$) correspond to the events that the desired link is LOS and NLOS and capture the effect of the coordination parameter ρ. Due to richer scattering of NLOS propagation, we usually have $M_{\mathrm{N}} < M_{\mathrm{L}}$ and thus

$$\begin{aligned}1-P_{\mathrm{PL}}(\theta) &\sim \Psi_{\mathrm{N}}(\rho)\theta^{M_{\mathrm{N}}}, \quad \theta\to 0,\\ 1-P_{\mathrm{PG}}(\theta) &\sim \tilde{\Psi}_{\mathrm{N}}(\rho)\theta^{M_{\mathrm{N}}}, \quad \theta\to 0.\end{aligned} \tag{38}$$

Hence, the success probabilities for different ρ are horizontally shifted versions (in dB) of each other, namely,

$$\begin{aligned}&1-P_{\mathrm{PL}}\big(\theta/\Psi_{\mathrm{N}}(\rho)^{1/M_{\mathrm{N}}}\big)\\ &\sim 1-P_{\mathrm{PL}}\big(\theta/\Psi_{\mathrm{N}}(0)^{1/M_{\mathrm{N}}}\big) \sim \theta^{M_{\mathrm{N}}}, \quad \theta\to 0,\\ &1-P_{\mathrm{PG}}\big(\theta/\widetilde{\Psi}_{\mathrm{N}}(\rho)^{1/M_{\mathrm{N}}}\big)\\ &\sim 1-P_{\mathrm{PG}}\big(\theta/\widetilde{\Psi}_{\mathrm{N}}(0)^{1/M_{\mathrm{N}}}\big) \sim \theta^{M_{\mathrm{N}}}, \quad \theta\to 0,\end{aligned} \tag{39}$$

where $\Psi_{\mathrm{N}}(0) = \widetilde{\Psi}_{\mathrm{N}}(0)$ is the pre-constant for no ICIC. Let

$$\begin{aligned}\kappa_{\mathrm{PL}}(\rho) &\triangleq \big(\Psi_{\mathrm{N}}(0)/\Psi_{\mathrm{N}}(\rho)\big)^{1/M_{\mathrm{N}}},\\ \kappa_{\mathrm{PG}}(\rho) &\triangleq \big(\widetilde{\Psi}_{\mathrm{N}}(0)/\widetilde{\Psi}_{\mathrm{N}}(\rho)\big)^{1/M_{\mathrm{N}}}\end{aligned} \tag{40}$$

be the asymptotic SIR gains with $\theta\to 0$ for the two proposed schemes, respectively. Based on the above asymptotic behavior, we further obtain an approximation to the success probability, given by

$$\begin{aligned}P_{\mathrm{PL}}(\theta \mid \rho=\rho_0) &\approx P_{\mathrm{PL}}(\theta/\kappa_{\mathrm{PL}}(\rho_0) \mid \rho=0),\\ P_{\mathrm{PG}}(\theta \mid \rho=\rho_0) &\approx P_{\mathrm{PG}}(\theta/\kappa_{\mathrm{PG}}(\rho_0) \mid \rho=0).\end{aligned} \tag{41}$$

Remark 3: The exact results require the calculation of the Laplace transform of the interference and its n-th derivative through numerical integration, and tedious and extensive computations make the exact calculation inefficient. Compared with the exact results, the approximate results merely require the computation of the exact success probability with $\rho=0$ (i.e., no ICIC) and the asymptotic SIR gains of different ρ. Since the computation of the asymptotic SIR gain merely requires a single numerical integration, this avoids the cumbersome evaluation of the exact results for different ρ and thus significantly simplifies the numerical evaluation. To further clarify the simplicity of the approximation, we consider the simple case with $M_{\mathrm{L}} = M_{\mathrm{N}} = 1$. For the exact success probabilities with different ρ, the following expression is numerically evaluated with nested integrals, given by

$$\begin{aligned}P_{\mathrm{PL}}(\theta) = &\sum_{k\in\{\mathrm{L,N}\}} \int_0^\infty f_k(r) \exp\Big(-2\pi\lambda \sum_{j\in\{\mathrm{m,s}\}} \sum_{i\in\{\mathrm{L,N}\}} w_j\\ &\times \int_{\left(\frac{r^{\alpha_k}}{1-\rho}\right)^{1/\alpha_i}}^\infty \frac{p_i(y) y \mathrm{d}y}{1+\theta^{-1}\frac{G_{\mathrm{m}}}{G_j}\frac{y^{\alpha_i}}{r^{\alpha_k}}}\Big)\mathrm{d}r,\end{aligned} \tag{42}$$

while for the approximation, the asymptotic SIR gain is numerically evaluated with single integrals, given by

$$\begin{aligned}&\kappa_{\mathrm{PL}}(\rho)\\ &= \frac{\int_0^\infty f_{\mathrm{N}}(r) r^{\alpha_{\mathrm{N}}} \Big(\sum_{j\in\{\mathrm{m,s}\}} \sum_{i\in\{\mathrm{L,N}\}} w_j G_j \chi_i(r^{\alpha_{\mathrm{N}}/\alpha_i}, \beta, 1)\Big)\mathrm{d}r}{\int_0^\infty f_{\mathrm{N}}(r) r^{\alpha_{\mathrm{N}}} \Big(\sum_{j\in\{\mathrm{m,s}\}} \sum_{i\in\{\mathrm{L,N}\}} w_j G_j \chi_i((\frac{r^{\alpha_{\mathrm{N}}}}{1-\rho})^{1/\alpha_i}, \beta, 1)\Big)\mathrm{d}r}.\end{aligned} \tag{43}$$

Hence the approximation is much simpler than the exact result in term of the computational complexity.

The asymptotic analysis of $\theta\to 0$ gives a simple approach to characterize the performance gain in the low-SIR regime, and the asymptotic gain merely depends on the NLOS component. For the high-SIR regime, we give an asymptotic expression as $\theta \to \infty$ in the following corollary.

Corollary 3. *For the two proposed schemes, the asymptotic SIR gains for $\theta \to \infty$ with $\rho < 1$ are 0 dB.*

Proof: Using the representation [28, Eqn. (18)] and following the Campbell-Mecke theorem [29, Thm. 8.2], the success probability with the PL-ICIC scheme when the desired link is LOS can be expressed as

$$\begin{aligned}P_{\mathrm{L}}(\theta) &= \mathbb{E}\sum_{x\in\Phi} p_{\mathrm{L}}(|x|)\bar{F}_h\Big[\frac{\theta|x|^{\alpha_{\mathrm{L}}}}{G_{\mathrm{m}}}\Big(\sum_{y\in\Phi\setminus\{x\}} G(\varphi_y)\chi_y\ell(y)h_y\Big)\Big]\\ &\quad\times\prod_{y\in\Phi\setminus\{x\}}\mathbf{1}_{|x|^{-\alpha_{\mathrm{L}}}>|y|^{-\alpha_y}}\\ &= \lambda\int_{\mathbb{R}^2}\mathbb{E}^{!o}\Big\{\bar{F}_h\Big[\frac{\theta|x|^{\alpha_{\mathrm{L}}}}{G_{\mathrm{m}}}\Big(\sum_{y\in\Phi_x} G(\varphi_y)\chi_y\ell(y)h_y\Big)\Big]\\ &\quad\times\prod_{y\in\Phi_x}\mathbf{1}_{|x|^{-\alpha_{\mathrm{L}}}>|y|^{-\alpha_y}}\Big\}p_{\mathrm{L}}(|x|)\mathrm{d}x, \qquad (44)\end{aligned}$$

where $\bar{F}_h$ is the complementary cumulative distribution function of the power fading coefficient, $\chi_y = 1 - \mathbf{1}_{(1-\rho)|x|^{-\alpha_{\mathrm{L}}}<|y|^{-\alpha_y}}$, and $\Phi_x \triangleq \{y\in\Phi\colon y+x\}$ is a translated version of Φ. Substituting $x\theta^{1/\alpha_{\mathrm{L}}}\mapsto x$ and letting $\Phi_x^\theta = \{y\in\Phi\colon y+x\theta^{-1/\alpha_{\mathrm{L}}}\}$, $\chi_y^\theta = 1-\mathbf{1}_{\theta(1-\rho)|x|^{-\alpha_{\mathrm{L}}}<|y|^{-\alpha_y}}$ and $I_\infty = \frac{1}{G_{\mathrm{m}}}\sum_{y\in\Phi}G(\varphi_y)\ell(y)h_y$, we have

$$\begin{aligned}P_{\mathrm{L}}(\theta) &= \lambda\theta^{-2/\alpha_{\mathrm{L}}}\int_{\mathbb{R}^2}\mathbb{E}^{!o}\Big\{\bar{F}_h\Big[\frac{|x|^{\alpha_{\mathrm{L}}}}{G_{\mathrm{m}}}\Big(\sum_{y\in\Phi_x^\theta}G(\varphi_y)\chi_y^\theta|y|^{-\alpha_k}h_y\Big)\Big]\\ &\quad\times\prod_{y\in\Phi_x^\theta}\mathbf{1}_{\theta|x|^{-\alpha_{\mathrm{L}}}>|y|^{-\alpha_y}}\Big\}p_{\mathrm{L}}(|x|\theta^{-1/\alpha_{\mathrm{L}}})\mathrm{d}x\\ &\overset{(a)}{\sim}\lambda\theta^{-2/\alpha_{\mathrm{L}}}\int_{\mathbb{R}^2}\mathbb{E}^{!o}\big[\bar{F}_h(|x|^{\alpha_{\mathrm{L}}}I_\infty)\big]\mathrm{d}x, \quad \theta\to\infty, \qquad (45)\end{aligned}$$

where step (a) follows from $\Phi_x^\theta \to \Phi$, $\chi_y^\theta \to 1$, $\mathbf{1}_{\theta|x|^{-\alpha_{\mathrm{L}}}>|y|^{-\alpha_y}} \to 1$ and $p_{\mathrm{L}}(|x|\theta^{-1/\alpha_{\mathrm{L}}}) \to 1$ as $\theta\to\infty$. It shows that $P_{\mathrm{L}}(\theta)$ does not depend on ρ as $\theta\to\infty$. A similar result holds when the desired link is NLOS and for the PG-ICIC scheme.

This shows that the asymptotic result of the success probability is the same as $\theta\to\infty$ for a finite ρ. Hence the asymptotic SIR gain for $\theta\to\infty$ is 0 dB. ■

Corollary 3 shows that the performance gain of the proposed ICIC schemes in the high-SIR regime is smaller than that in the low-SIR regime and vanishes as $\theta\to\infty$. It is interpreted as follows: for a high SIR threshold, the interfering BSs with weak interference might not be muted by the ICIC schemes but still cause the failure of the transmission, and hence the proposed ICIC schemes have a weaker impact on the success probability with a high SIR threshold. When θ is large, a successful transmission is only possible if all interfering BSs are far away from the served user, and there is already no interfering BS in the guard zone for $\rho < 1$, and no BS needs to be muted. Hence the performance gain of the proposed ICIC schemes vanishes.

D. Normalized Throughput

Although both ICIC schemes improve the success probability at the typical user, the serving BS needs to mute some RBs required by other BSs and the muted RBs cannot be used to transmit data to users. Since the success probability of the typical (served) user does not capture this effect, we define a novel metric, termed *normalized throughput*, that accounts for the fact that some RBs are no longer used to serve other users. It is defined as

$$\xi(\theta) \triangleq \mathbb{E}\Big[\frac{\mathbf{1}_{\mathrm{SIR}>\theta}}{1+\zeta}\Big], \qquad (46)$$

where ζ is the number of the RBs muted at the serving BS due to requests by other BSs. The normalized throughput can be interpreted as the (local) throughput divided by the rate of transmission, which is similar to the concepts of the probabilistic throughput in [31] and the normalized spectral efficiency in [32]. The normalized throughput captures the overall performance, which takes into account that fewer users can be served if some RBs are muted, while the success probability of the typical user reflects the user-perceived performance if the user is served by its BS. Since both SIR and ζ strongly depend on the spatial distributions of BSs and their serving users, a complicated correlation is introduced into the analysis of the normalized throughput. Moreover, the analysis of ζ involves the distance distributions between other BSs and their users and the distance distributions between other BSs and the serving BS of the typical user, which is a challenging task due to the interaction between multiple BSs. To tackle these issues, we propose to first approximate the normalized throughput with an independence assumption between the SIR and ζ, and further approximate ζ by the total number of the muted RBs of other BSs as requested by the serving BS of the typical user, denoted by $\tilde{\zeta}$, which is equal to the number of BSs in the coordinated set.

Definition 1. *The approximate normalized throughput (ANT) is defined as the product of the success probability and the expected value of the reciprocal of the total number of BSs participating in the coordination for the typical user, expressed by*

$$\tilde{\xi}(\theta) \triangleq \mathbb{E}\mathbf{1}_{\mathrm{SIR}>\theta}\,\mathbb{E}\Big[\frac{1}{1+\tilde{\zeta}}\Big]. \qquad (47)$$

In the following, we analyze the ANTs of both schemes.

Theorem 3. *The ANT of the PL-ICIC scheme is given by*

$$\tilde{\xi}_{\mathrm{PL}}(\theta) = P_{\mathrm{PL}}(\theta)\sum_{k\in\{\mathrm{L},\mathrm{N}\}}\int_0^\infty f_k(r)\frac{1-e^{-\omega_k(r)}}{\omega_k(r)}\mathrm{d}r, \qquad (48)$$

where

$$\begin{aligned}\omega_k(r) &= \frac{2\pi\lambda}{\beta^2}\Big(e^{-\beta r^{\alpha_k/\alpha_{\mathrm{L}}}}(1+\beta r^{\alpha_k/\alpha_{\mathrm{L}}})\\ &\quad+e^{-\beta\bar{r}_{k,\mathrm{N}}}(1+\beta\bar{r}_{k,\mathrm{N}}) - e^{-\beta\bar{r}_{k,\mathrm{L}}}(1+\beta\bar{r}_{k,\mathrm{L}})\\ &\quad-e^{-\beta r^{\alpha_k/\alpha_{\mathrm{N}}}}(1+\beta r^{\alpha_k/\alpha_{\mathrm{N}}})\Big) + \pi\lambda(\bar{r}_{k,\mathrm{N}}^2 - r^{2\alpha_k/\alpha_{\mathrm{N}}}).\end{aligned} \qquad (49)$$

Proof: See Appendix B.

TABLE I. Symbols and descriptions

Symbol	Description	Default value
Φ, λ	The mm-wave BS PPP and density	$\mathrm{N/A}, 5 \times 10^{-4}$
β	The parameter to characterize the blockage effect	0.01
$\alpha_{\mathrm{L}}/\alpha_{\mathrm{N}}$	The path loss exponent of the LOS/NLOS link	$2.5/4$
$M_{\mathrm{L}}/M_{\mathrm{N}}$	The fading parameter of the LOS/NLOS link	$4/2$
N	The antenna array size of the ULA	32
$G_{\mathrm{m}}/G_{\mathrm{s}}$	The main lobe/side lobe gain of the antenna pattern	N/A
w_{m}	The beam-width of the antenna pattern	N/A
ρ	The coordination level parameter of the ICIC scheme	0.96
θ	The SIR threshold	N/A
$P(\theta)$	The success probability	N/A
$\xi(\theta)/\tilde{\xi}(\theta)$	The normalized throughput/the approximate normalized throughput	N/A

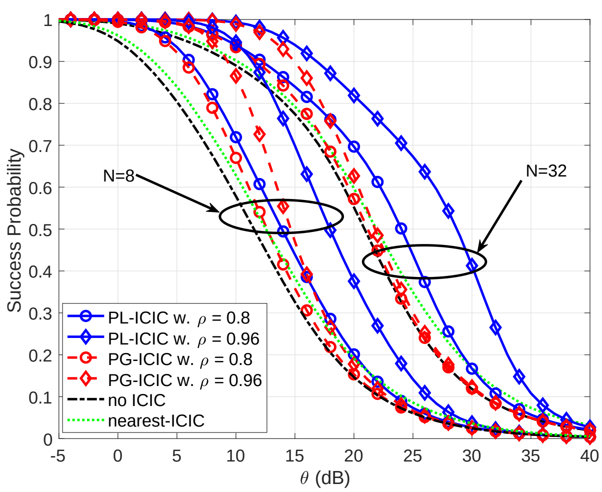

Fig. 1. The success probabilities for different ICIC schemes.

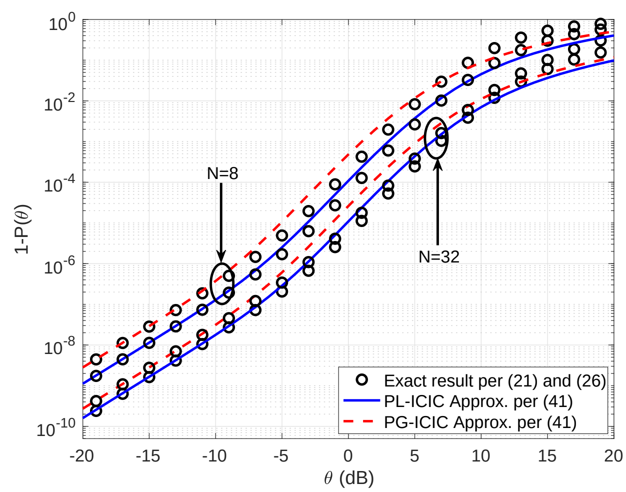

Fig. 2. The approximation of the outage probabilities $1 - P(\theta)$ for different ICIC schemes.

Theorem 4. *The ANT of the PG-ICIC scheme is given by*

$$\tilde{\xi}_{\mathrm{PG}}(\theta) = P_{\mathrm{PG}}(\theta) \sum_{k\in\{\mathrm{L,N}\}} \int_0^\infty f_k(r) \frac{1 - e^{-\widetilde{\omega}_k(r)}}{\widetilde{\omega}_k(r)} \mathrm{d}r, \quad (50)$$

where

$$\widetilde{\omega}_k(r) = 2\pi\lambda \sum_{j\in\{\mathrm{m,s}\}} \frac{w_j}{\beta^2} \Big(e^{-\beta r^{\alpha_k/\alpha_{\mathrm{L}}}} (1 + \beta r^{\alpha_k/\alpha_{\mathrm{L}}}) + e^{-\beta \tilde{r}_{k,\mathrm{N},j}} (1 + \beta \tilde{r}_{k,\mathrm{N},j}) - e^{-\beta \tilde{r}_{k,\mathrm{L},j}} (1 + \beta \tilde{r}_{k,\mathrm{L},j}) - e^{-\beta r^{\alpha_k/\alpha_{\mathrm{N}}}} (1 + \beta r^{\alpha_k/\alpha_{\mathrm{N}}}) \Big) + \frac{w_j}{2} (\tilde{r}_{k,\mathrm{N},j}^2 - r^{2\alpha_k/\alpha_{\mathrm{N}}}). \quad (51)$$

Proof: The proof is analogous to that of Theorem 3, with a modified spatial distribution of the interfering BSs according to the coordinating set Ω_{PG}. ■

IV. Numerical Results

In this section, we present numerical results of the success probability and the normalized throughput for mm-wave cellular networks with the two BS muting schemes. We also compare them with the simulation results of a common ICIC scheme where the nearest interfering BS to the typical user is muted (abbreviated as nearest-ICIC). The main symbols and parameters are summarized in Table I and default values are given where applicable.

Fig. 1 compares the success probabilities of the two ICIC schemes with different ρ and antenna size N. It is observed that the PL-ICIC scheme outperforms the PG-ICIC scheme in all cases, which results from that more RBs are muted in the PL-ICIC scheme. We also observe that the performance gap between the two ICIC schemes becomes larger when ρ or N become larger. For instance, given that the success probability is 0.6, the horizontal gaps in the case of $N = 32$ between the two schemes with $\rho = 0.8$ and $\rho = 0.96$ are 2.7 dB and 6.6 dB, respectively, and the horizontal gaps in the case of $\rho = 0.96$ between the two schemes with $N = 8$ and $N = 32$ are 3 dB and 6.6 dB, respectively. This is because larger ρ and N magnify the area gap between the coordinating regions Ω_{PL} and Ω_{PG} and thus lead to a corresponding performance gap. It is seen that the performance gains of the two proposed ICIC schemes over no ICIC become larger as θ decreases, which shows the advantage of the proposed ICIC schemes in the low-SIR regime (the regime with low SIR requirements). The larger the number of antennas, the wider the range of θ for which there is an improvement. For instance, when $N = 8$, there is performance improvement over no ICIC for $\theta < 30$ dB, and when $N = 32$, for $\theta < 40$ dB. Compared with the nearest-ICIC scheme, the proposed two schemes are better in

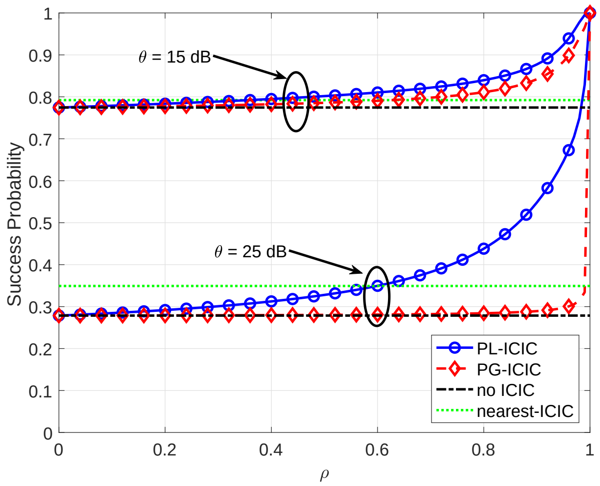

Fig. 3. The success probability versus the coordination parameter with $N = 32$.

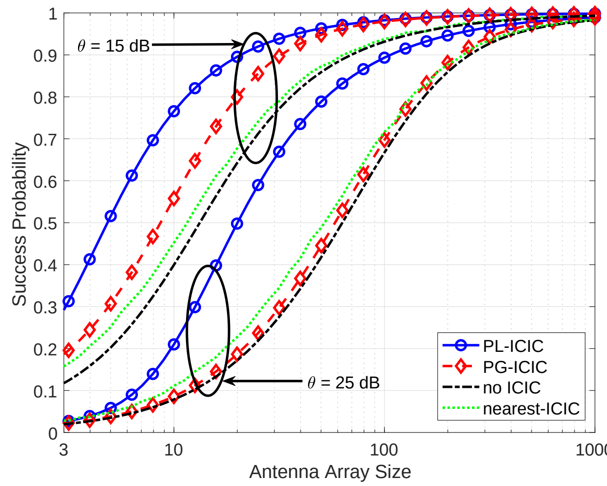

Fig. 4. The success probability versus the antenna array sizes.

the low-SIR regime (because the nearest interfering BS is not always the strongest interfering BS), but slightly worse in the high-SIR regime, because the nearest-ICIC scheme certainly mutes one RB of the nearest interfering BS while the proposed two schemes do not.

Fig. 2 shows the comparison between the exact success probability and the proposed approximative result based on the asymptotic SIR gain at $\theta \to 0$. It can be seen that the approximations are close to the exact results in a wide range of θ and match the exact result well in the low-SIR regime $\theta < -13$ dB, which shows the effectiveness of the proposed approximation. As θ increases, the deviation of the approximation becomes larger, which means the proposed approximation is less suitable for the high-SIR regime. This is consistent with the asymptotic analysis of $\theta \to \infty$, where the SIR gain vanishes. We also observe that the antenna array size affects the range of an accurate approximation, where the deviation starts at $\theta = -11$ dB and $\theta = -7$ dB for $N = 8$ and $N = 32$, respectively.

Fig. 3 shows the relationship between the success probability and the coordination parameter ρ with $N = 32$. Compared with no ICIC, the PL-ICIC scheme smoothly achieves a better success probability with the increasing ρ for the two SIR thresholds, and the PG-ICIC scheme behaves similarly and provides a comparable performance with the PL-ICIC scheme for $\theta = 15$ dB. However, for $\theta = 25$ dB, as ρ increases, the success probability of the PG-ICIC scheme is almost the same as in the no ICIC scheme when $\rho < 0.88$ and then presents a sharp performance improvement. This shows that the side lobe interference causes a significant performance degradation in the case with a large SIR threshold requirement and hence a large ρ is needed to mute these interfering BSs with the side lobe pointing to the target user. Compared with the nearest-ICIC scheme, the proposed two schemes yield a better performance with a larger ρ while a worse performance with a smaller ρ, and the smaller the SIR requirement, the wider the range of ρ for which there is an improvement. Furthermore, we also observe that the performance gap between the two scheme grows with the increase of ρ until the success probability reaches 1.

Fig. 4 shows the impact of the antenna size N on the success probability. We also observe that for a fixed N, a bigger improvement in the success probability is achieved with a lower SIR threshold for both ICIC schemes. The gap between the success probabilities of both schemes grows first and then declines with the increase of N. Furthermore, the success probabilities of all schemes tend to be consistent with that of no ICIC when N is larger than 500. This is because the narrow beams of the large antenna arrays cause negligible interference to the target user, and thus all ICIC schemes nearly have the same impact on the interference. Compared with the nearest-ICIC scheme, the two proposed ICIC schemes provide a better reliability for a small SIR threshold while merely the PL-ICIC scheme is better for a large SIR threshold, which again shows the advantage of the two proposed schemes in the low SIR regime.

Fig. 5 shows how the success probability varies with the LOS parameter β with $N = 32$. We observe that the success probabilities of the two proposed ICIC schemes increases with increasing β and then decreases after reaching a peak value. The reason is that a worse LOS propagation environment (i.e., smaller LOS probability with larger β) yields a weaker desired signal strength and less interference to the target user, and hence the increasing β shows a competing impact on the success probability. In the early stage of increasing β, the reduced interference has a dominant impact and thus improves the performance. As β increases, the desired link experiences the NLOS propagation environment with higher probability and thus the performance degrades even though the interference is also reduced. Comparing the three ICIC schemes, the nearest-ICIC provides the worst performance for a small SIR threshold while lies in between the two proposed schemes.

Fig. 6 shows the accuracy of the approximate normalized throughput of different coordination parameters ρ with $N = 32$ and $\theta = 15$ dB, where the simulation results show the actual

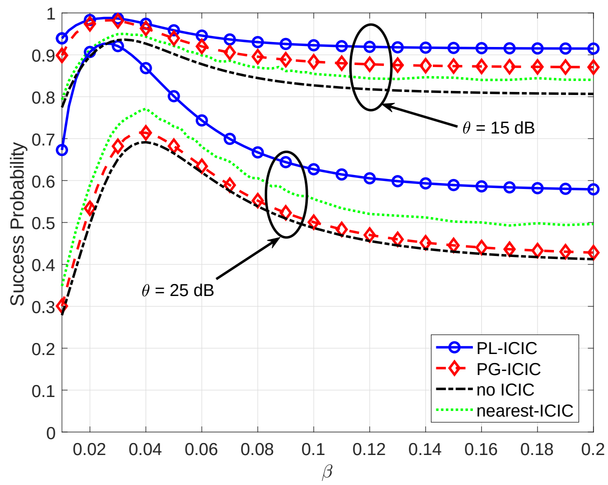

Fig. 5. The success probability versus the LOS parameter β with $N = 32$ and $\rho = 0.95$.

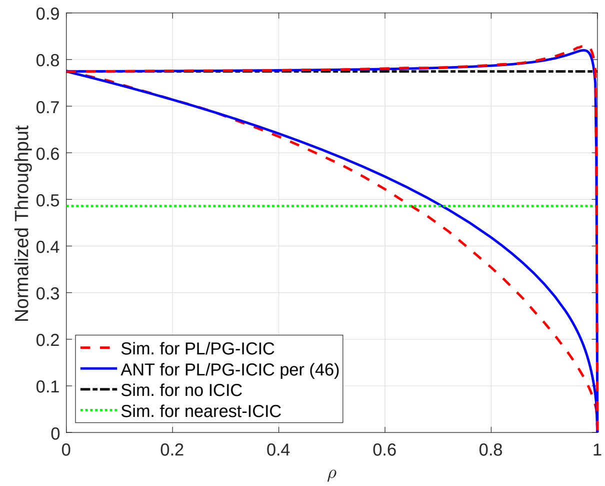

Fig. 6. The validation of the ANT with $N = 32$ and $\theta = 15$ dB.

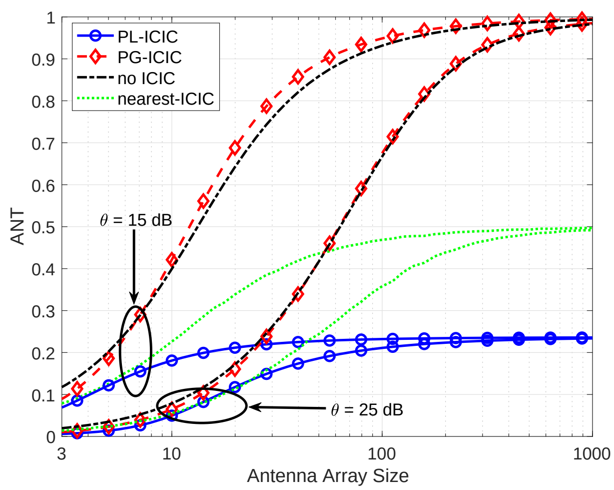

Fig. 7. The ANT versus the antenna array size.

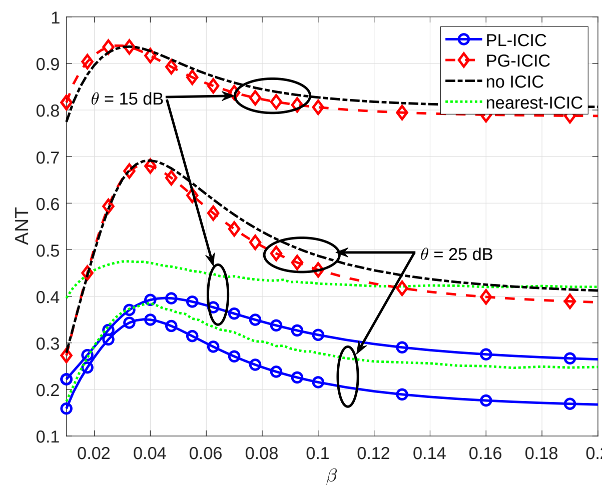

Fig. 8. The ANT versus the LOS parameter β.

normalized throughput. We observe that the approximation matches well with the simulation result in the PG-ICIC scheme and accurately reflects the trend in the PL-ICIC scheme, which verifies the effectiveness of the proposed approximation. As ρ increases, the normalized throughput of the PL-ICIC scheme is always lower than that of no ICIC (i.e., $\rho = 0$) and becomes smaller, while the normalized throughput of the PG-ICIC scheme first increases to a peak value slowly and then declines. Hence, there is a certain range of ρ where the PG-ICIC scheme is better than no ICIC. In comparison with the nearest-ICIC scheme, the PL-ICIC scheme gives a lower normalized throughput for $\rho > 0.65$ and PG-ICIC scheme for ρ nearly reaching 1 (i.e., full coordination). This is because the nearest-ICIC scheme always pays the price of one muted interfering BS while the proposed two schemes mute more BSs for a larger ρ. These observations show the advantage of the PG-ICIC scheme on the overall network performance in the high coordination level (i.e., large ρ).

Fig. 7 shows the impact of the antenna array size N on the ANT, where the ANT of the nearest-ICIC scheme is $0.5P(\theta)$ obtained via simulations. As seen in the figure, the PG-ICIC scheme outperforms the PL-ICIC and nearest-ICIC schemes for different antenna array sizes. As the antenna array size increases, we observe that the ANT of the PG-ICIC scheme tends to that without ICIC and both tend to 1. The reason is that the increasing N yields fewer muted RBs of other BSs in the PG-ICIC scheme and the number tends to 0 as $N \to \infty$. Furthermore, as N increases, the antenna gain of the desired link is enhanced and the inter-cell interference is significantly reduced due to the narrower beam, thus the ANT tends to 1. Compared with the PL-ICIC and nearest schemes, the advantage of the PG-ICIC scheme becomes more apparent with the increase of N. The ANT of the PL-ICIC scheme tends to a value less than 1 (0.23 in this case), because it is limited by the number of the muted RBs, which does not depend on the antenna array size. The ANT of the nearest-ICIC scheme tends to 0.5, because there is always one muted RB of the closest interfering BS.

Fig. 8 shows how the LOS parameter affects the ANT with $N = 32$. For varying LOS parameters, the overall performance of the PG-ICIC scheme is close to that without ICIC but much better than the PL-ICIC and nearest-ICIC schemes, and we can also observe that the PG-ICIC scheme achieves a better normalized throughput for $\theta = 15$ dB when $\beta < 0.03$, which shows the effectiveness of the PG-ICIC scheme in terms of the overall performance.

V. Concluding Remarks

In this paper, we proposed two ICIC schemes for mm-wave cellular networks, where the coordinating BSs are muted under consideration of the unique characteristics (blockage effect and directional transmission) of mm-wave communications. To fully characterize the ICIC technique in mm-wave cellular networks, we provided analytical expressions of the performance metrics in terms of success probability and approximate normalized throughput with the aid of stochastic geometry. To efficiently evaluate the performance gain of the two proposed ICIC schemes, the asymptotic analyses of the success probability for $\theta \to 0$ and ∞ are given, which show that the two proposed ICIC schemes yield a significant performance gain in the low-SIR regime while the gain vanishes as the SIR threshold tends to infinity. Based on the asymptotic analysis, we further propose a simple approximative approach to evaluate success probability and characterize the performance gain of the ICIC schemes. Numerical results demonstrate that the proposed two ICIC schemes significantly improve the success probability of the users served by their BSs for mm-wave networks. Meanwhile, the PL-ICIC scheme yields a better success probability than PG-ICIC scheme with more muted resource blocks of coordinated BSs and thus leads to worse normalized throughput. Hence, the PL-ICIC scheme is suitable in scenarios with ultra-high reliability requirements and light load while the PG-ICIC scheme is effective in the scenarios with medium/high-reliability and heavy load. In summary, the proposed ICIC schemes and the corresponding theoretical results help understand how to improve the user-perceived performance and trade it off with the cost incurred when mm-wave networks perform coordination among BSs.

Appendix A
Proof of Theorem 1

Proof: Letting $I = \sum_{x\in\Phi^!} G(\varphi_x)h_x\chi_x\ell(x)$, the success probability of PL-ICIC is given by

$$\begin{aligned}
P_{\rm PL}(\theta) &= \sum_{k\in\{\mathrm{L,N}\}} A_k \mathbb{P}\left(\frac{G_{\rm m} h_{x_0} r_0^{-\alpha_k}}{I} > \theta\right)\\
&= \sum_{k\in\{\mathrm{L,N}\}} A_k \mathbb{E}\left[\widetilde{\Gamma}\left(M_k, \tilde{\theta}_k r_0^{\alpha_k} I\right)\right]\\
&= \sum_{k\in\{\mathrm{L,N}\}} A_k \sum_{l=0}^{M_k-1} \mathbb{E}\left[e^{-\tilde{\theta}_k r_0^{\alpha_k} I}\frac{(\tilde{\theta}_k r_0^{\alpha_k} I)^l}{l!}\right]\\
&= \sum_{k\in\{\mathrm{L,N}\}} \sum_{l=0}^{M_k-1} \int_0^\infty f_k(r)\frac{(-u)^l}{l!}\mathcal{L}_k^{(l)}(r,u)|_{u=\tilde{\theta}_k r^{\alpha_k}}\mathrm{d}r,
\end{aligned}$$

where $\tilde{\theta}_k = \frac{\theta M_k}{G_{\rm m}}$, $\widetilde{\Gamma}(x,y) = \Gamma(x,y)/\Gamma(x)$ is the normalized incomplete gamma function, $\mathcal{L}_k(r,u) = \mathbb{E}[e^{-uI}]$ is the Laplace transform of I under the condition that the serving BS x_0 is at a distance r and x_0 is LOS ($k = \mathrm{L}$) or NLOS ($k = \mathrm{N}$), and the superscript (m) stands for the m-th derivative of $\mathcal{L}_k(r,u)$ w.r.t. u. The spatial distributions of the interferers are different in two cases that the serving BS is either LOS or NLOS, which affects $\mathcal{L}_k(r,u)$. When $x_0 \in \Phi_{\rm L}$ and $x_0 = r$, the interference powers from LOS and NLOS BSs are expressed as

$$I(r) = \sum_{x\in\Phi^!\setminus\Omega_{\rm PL}} G(\varphi_x)h_x|x|^{-\alpha_x}. \tag{52}$$

From Slivnyak's theorem [29], $\Phi^!$ remains the same as the original PPP Φ. Then we have

$$\begin{aligned}
&\mathcal{L}_{\rm L}(r,u)\\
&= \prod_{i\in\{\mathrm{L,\,N}\}} \mathbb{E}\exp\big(-uI(r)\big)\\
&= \mathbb{E}\left[\prod_{x\in\Phi\setminus\Omega_{\rm PL}}\left(\sum_{i\in\{\mathrm{L,N}\}}\frac{p_i(|x|)}{\big(1+\frac{uG(\varphi_x)|x|^{-\alpha_i}}{M_i}\big)^{M_i}}\right)\right]\\
&= \mathbb{E}\left[\prod_{x\in\Phi\setminus\Omega_{\rm PL}}\left(\sum_{i\in\{\mathrm{L,N}\}}\sum_{j\in\{\mathrm{m,s}\}}\frac{w_j p_i(|x|)}{\Big(1+\frac{uG_j|x|^{-\alpha_i}}{M_i}\Big)^{M_i}}\right)\right]\\
&\overset{(a)}{=}\exp\left(-2\pi\lambda\sum_{j\in\{\mathrm{m,s}\}}\sum_{i\in\{\mathrm{L,N}\}} w_j\right.\\
&\qquad\left.\times\int_{\bar{r}_{\mathrm{L},i}}^\infty\left(1-\frac{1}{\big(1+\frac{uG_j y^{-\alpha_i}}{M_i}\big)^{M_i}}\right)p_i(y)y\mathrm{d}y\right),
\end{aligned}\tag{53}$$

where step (a) follows from the probability generating functional (PGFL) of the PPP [29] and the lower integration limit is obtained since the closest interferer is at least at a distance $\bar{r}_{\mathrm{L},i} = (1-\rho)^{-1/\alpha_i} r^{\alpha_{\rm L}/\alpha_i}$ obtained from the coordinating set $\Omega_{\rm PL}$. Letting

$$\begin{aligned}
\eta_k(r,u) = &-2\pi\lambda\sum_{j\in\{\mathrm{m,s}\}}\sum_{i\in\{\mathrm{L,N}\}} w_j\\
&\times\int_{\bar{r}_{k,i}}^\infty\left(1-\frac{1}{\big(1+\frac{uG_j y^{-\alpha_i}}{M_i}\big)^{M_i}}\right)p_i(y)y\mathrm{d}y,
\end{aligned}\tag{54}$$

we have $\mathcal{L}_{\rm L}(r,u) = \exp\big(\eta_{\rm L}(r,u)\big)$. Since $\mathcal{L}_{\rm L}^{(1)}(r,u) = \eta^{(1)}(r,u)\mathcal{L}_{\rm L}(r,u)$, $\mathcal{L}_{\rm L}^{(l)}(r,u)$ can be calculated recursively according to the formula of Leibniz, given by

$$\mathcal{L}_{\rm L}^{(l)}(r,u) = \sum_{n=0}^{l-1}\binom{l-1}{n}\eta^{(l-n)}(r,u)\mathcal{L}_{\rm L}^{(n)}(r,u), \tag{55}$$

where the n-th derivative of $\eta_{\rm L}(r,u)$ w.r.t. u is

$$\begin{aligned}
\eta_{\rm L}^{(n)}(r,u) = &\,2\pi\lambda\sum_{j\in\{\mathrm{m,s}\}}\sum_{i\in\{\mathrm{L,N}\}} w_j\big(-\frac{G_j}{M_i}\big)^n\frac{\Gamma(M_i+n)}{\Gamma(M_i)}\\
&\times\int_{\bar{r}_{\mathrm{L},i}}^\infty\frac{p_i(y)y^{1-n\alpha_i}}{\big(1+\frac{uG_j y^{-\alpha_i}}{M_i}\big)^{M_i+n}}\mathrm{d}y.
\end{aligned}\tag{56}$$

When $x_0 \in \Phi_{\rm N}$ and $x_0 = r$, we derive $\mathcal{L}_{\rm N}(r,u) = \exp\big(\eta_{\rm N}(r,u)\big)$ and its derivatives analogously. ■

Appendix B
Proof of Theorem 3

Proof: The ANT with the PL-ICIC scheme is

$$\begin{aligned}\tilde{\xi}_{\rm PL}(\theta) &= \tilde{\xi}(\theta) = \mathbb{E}\mathbf{1}_{\rm SIR>\theta}\,\mathbb{E}\Big[\frac{1}{1+\tilde{\zeta}}\Big]\\ &= P_{\rm PL}(\theta)\mathbb{E}\Big[\frac{1}{1+\tilde{\zeta}}\Big]\\ &= P_{\rm PL}(\theta)\int_0^R f_k(r)\underbrace{\mathbb{E}\Big[\frac{1}{1+\zeta}\mid r_0=r\Big]}_{\mathcal{X}_k(r)}\mathrm{d}r, \quad (57)\end{aligned}$$

where $\mathcal{X}_k(r)$ characterizes the cost for coordinating the information transmission under the condition that $|x_0| = r_0$ and x_0 belongs to Φ_k, $k \in \{\mathrm{L},\mathrm{N}\}$. Letting $\tilde{\zeta}_{\rm L}$ and $\tilde{\zeta}_{\rm N}$ be the total number of the muted RBs of LOS and NLOS BSs, respectively, we have $\tilde{\zeta} = \tilde{\zeta}_{\rm L}+\tilde{\zeta}_{\rm N}$, and according to the desired BS belonging to LOS or NLOS, the following two disjoint events are considered.

One is conditioning on $x_0 \in \Phi_{\rm L}$ and $|x_0| = r$. In this case, an RB of each LOS BS $x \in \Phi_{\rm L}$ are muted for the typical user under the PL-ICIC scheme if $r < |x| < (1-\rho)^{-1/\alpha_{\rm L}}r$, and thus $\zeta_{\rm L}$ follows a Poisson distribution with mean, given by

$$\begin{aligned}\mathbb{E}\tilde{\zeta}_{\rm L} &= \mathbb{E}\Big[\sum_{x\in\Phi_{\rm L}}\mathbf{1}_{r<|x|<r(1-\rho)^{-1/\alpha_{\rm L}}}\Big]\\ &= 2\pi\lambda\int_r^{r(1-\rho)^{-1/\alpha_{\rm L}}} p_{\rm L}(r)r\mathrm{d}r\\ &= 2\pi\lambda\big(\phi_{\rm L}(\bar{r}_{\rm L,L},\beta)-\phi_{\rm L}(r,\beta)\big), \quad (58)\end{aligned}$$

where

$$\phi_{\rm L}(x,\beta) = \int_0^x e^{-\beta r}r\mathrm{d}r = \frac{1}{\beta^2}-e^{-\beta x}. \quad (59)$$

An RB of each NLOS BS $x \in \Phi_{\rm N}$ is muted if $r^{\alpha_{\rm L}/\alpha_{\rm N}} < |x| < (1-\rho)^{-1/\alpha_{\rm N}}r^{\alpha_{\rm L}/\alpha_{\rm N}}$, and $\zeta_{\rm N}$ also follows a Poisson distribution with mean $\mathbb{E}\zeta_{\rm N} = 2\pi\lambda\big(\phi_{\rm N}(\bar{r}_{\rm L,N},\beta)-\phi_{\rm N}(r^{\alpha_{\rm L}/\alpha_{\rm N}},\beta)\big)$, where

$$\begin{aligned}\phi_{\rm N}(x,\beta) &= \int_0^x(1-e^{-\beta r})r\mathrm{d}r\\ &= \frac{x^2}{2}-\frac{1}{\beta^2}+e^{-\beta x}\frac{1+x\beta}{\beta^2}. \quad (60)\end{aligned}$$

Given that $x_0 \in \Phi_{\rm L}$ and $|x_0| = r$, $\zeta_{\rm L}$ and $\zeta_{\rm N}$ are independent, and thus ζ follows a Poisson distribution with mean

$$\omega_{\rm L}(r) = 2\pi\lambda\sum_{i\in\{\mathrm{L},\mathrm{N}\}}\big(\phi_i(\bar{r}_{{\rm L},i},\beta)-\phi_i(r^{\alpha_{\rm L}/\alpha_i},\beta)\big), \quad (61)$$

and we further obtain

$$\begin{aligned}\mathcal{X}_{\rm L}(r) &= \sum_{n=0}^{\infty}\frac{1}{1+n}e^{-\omega_{\rm L}(r)}\frac{(\omega_{\rm L}(r))^n}{n!}\\ &= \frac{e^{-\omega_{\rm L}(r)}}{\omega_{\rm L}(r)}\sum_{n=0}^{\infty}\frac{(\omega_{\rm L}(r))^{n+1}}{(n+1)!}\\ &= \frac{1-e^{-\omega_{\rm L}(r)}}{\omega_{\rm L}(r)}. \quad (62)\end{aligned}$$

The other is conditioning on $x_0 \in \Phi_{\rm N}$ and $|x_0| = r$. In this case, ζ follows a Poisson distribution with mean

$$\omega_{\rm N}(r) = 2\pi\lambda\sum_{i\in\{\mathrm{L},\mathrm{N}\}}\big(\phi_i(\bar{r}_{{\rm N},i},\beta)-\phi_i(r^{\alpha_{\rm N}/\alpha_i},\beta)\big), \quad (63)$$

and $\omega_{\rm N}(r)$ is derived analogously, given by

$$\mathcal{X}_{\rm N}(r) = \frac{1-e^{-\omega_{\rm N}(r)}}{\omega_{\rm N}(r)}. \quad (64)$$

The final result is obtained by substituting (59), (60), (62) and (64) into (57). ■

References

[1] H. Wei, N. Deng, and M. Haenggi, "Inter-cell interference coordination in millimeter-wave cellular networks," in *IEEE Global Communications Conference (GLOBECOM'19)*, Waikaloa, HI, USA, Dec. 2019.

[2] Z. Pi and F. Khan, "An introduction to millimeter-wave mobile broadband systems," *IEEE Communications Magazine*, vol. 49, no. 6, pp. 101–107, Jun. 2011.

[3] F. Boccardi, R. W. Heath, A. Lozano, T. L. Marzetta, and P. Popovski, "Five disruptive technology directions for 5G," *IEEE Communications Magazine*, vol. 52, no. 2, pp. 74–80, Feb. 2014.

[4] T. S. Rappaport, S. Sun, R. Mayzus, H. Zhao, Y. Azar, K. Wang, G. N. Wong, J. K. Schulz, M. Samimi, and F. Gutierrez, "Millimeter wave mobile communications for 5G cellular: It will work!" *IEEE Access*, vol. 1, pp. 335–349, 2013.

[5] X. Yu, J. Zhang, M. Haenggi, and K. B. Letaief, "Coverage analysis for millimeter wave networks: The impact of directional antenna arrays," *IEEE Journal on Selected Areas in Communications*, vol. 35, no. 7, pp. 1498–1512, Jul. 2017.

[6] N. Deng and M. Haenggi, "A fine-grained analysis of millimeter-wave device-to-device networks," *IEEE Transactions on Communications*, vol. 65, no. 11, pp. 4940–4954, Nov. 2017.

[7] Y. Li, E. Pateromichelakis, N. Vucic, J. Luo, W. Xu, and G. Caire, "Radio resource management considerations for 5G millimeter wave backhaul and access networks," *IEEE Communications Magazine*, vol. 55, no. 6, pp. 86–92, Jun. 2017.

[8] H. Shokri-Ghadikolaei, F. Boccardi, C. Fischione, G. Fodor, and M. Zorzi, "Spectrum sharing in mmwave cellular networks via cell association, coordination, and beamforming," *IEEE Journal on Selected Areas in Communications*, vol. 34, no. 11, pp. 2902–2917, Nov. 2016.

[9] W. Feng, Y. Wang, D. Lin, N. Ge, J. Lu, and S. Li, "When mmwave communications meet network densification: A scalable interference coordination perspective," *IEEE Journal on Selected Areas in Communications*, vol. 35, no. 7, pp. 1459–1471, Jul. 2017.

[10] W. Zhang, Y. Wei, S. Wu, W. Meng, and W. Xiang, "Joint beam and resource allocation in 5G mmWave small cell systems," *IEEE Transactions on Vehicular Technology*, vol. 68, no. 10, pp. 10 272–10 277, Oct. 2019.

[11] P. Zhou, X. Fang, X. Wang, Y. Long, R. He, and X. Han, "Deep learning-based beam management and interference coordination in dense mmwave networks," *IEEE Transactions on Vehicular Technology*, vol. 68, no. 1, pp. 592–603, Jan. 2019.

[12] R. Kim, Y. Kim, N. Y. Yu, S. Kim, and H. Lim, "Online learning-based downlink transmission coordination in ultra-dense millimeter wave heterogeneous networks," *IEEE Transactions on Wireless Communications*, vol. 18, no. 4, pp. 2200–2214, Apr. 2019.

[13] N. Deng, M. Haenggi, and Y. Sun, "Millimeter-wave device-to-device networks with heterogeneous antenna arrays," *IEEE Transactions on Communications*, vol. 66, no. 9, pp. 4271–4285, Sep. 2018.

[14] E. Turgut and M. C. Gursoy, "Uplink performance analysis in D2D-enabled millimeter-wave cellular networks with clustered users," *IEEE Transactions on Wireless Communications*, vol. 18, no. 2, pp. 1085–1100, Feb. 2019.

[15] J. Fan, L. Han, X. Luo, Y. Zhang, and J. Joung, "Beamwidth design for beam scanning in millimeter-wave cellular networks," *IEEE Transactions on Vehicular Technology*, vol. 69, no. 1, pp. 1111–1116, Jan. 2020.

[16] Y. Zhu, G. Zheng, and K. Wong, "Stochastic geometry analysis of large intelligent surface-assisted millimeter wave networks," *IEEE Journal on Selected Areas in Communications*, vol. 38, no. 8, pp. 1749–1762, Aug. 2020.

[17] C. Skouroumounis, C. Psomas, and I. Krikidis, “Low-complexity base station selection scheme in mmwave cellular networks,” *IEEE Transactions on Communications*, vol. 65, no. 9, pp. 4049–4064, Sep. 2017.
[18] D. Maamari, N. Devroye, and D. Tuninetti, “Coverage in mmWave cellular networks with base station co-operation,” *IEEE Transactions on Wireless Communications*, vol. 15, no. 4, pp. 2981–2994, Apr. 2016.
[19] H. Wang, K. Huang, and T. A. Tsiftsis, “Base station cooperation in millimeter wave cellular networks: Performance enhancement of cell-edge users,” *IEEE Transactions on Communications*, vol. 66, no. 11, pp. 5124–5139, Nov. 2018.
[20] 3GPP, “Evolved universal terrestrial radio access (E-UTRA): X2 application protocol (X2AP),” 3rd Generation Partnership Project (3GPP), Technical Specification (TS) 36.423, Sep. 2018, version 15.3.0.
[21] X. Zhang and M. Haenggi, “A stochastic geometry analysis of inter-cell interference coordination and intra-cell diversity,” *IEEE Transactions on Wireless Communications*, vol. 13, no. 12, pp. 6655–6669, Dec. 2014.
[22] J. Yoon and G. Hwang, “Distance-based inter-cell interference coordination in small cell networks: Stochastic geometry modeling and analysis,” *IEEE Transactions on Wireless Communications*, vol. 17, no. 6, pp. 4089–4103, Jun. 2018.
[23] H. Wang, S. Leung, and R. Song, “Uplink area spectral efficiency analysis for multichannel heterogeneous cellular networks with interference coordination,” *IEEE Access*, vol. 6, pp. 14 485–14 497, 2018.
[24] J. Park, J. G. Andrews, and R. W. Heath, “Inter-operator base station coordination in spectrum-shared millimeter wave cellular networks,” *IEEE Transactions on Cognitive Communications and Networking*, vol. 4, no. 3, pp. 513–528, Sep. 2018.
[25] T. Bai, R. Vaze, and R. W. Heath, “Analysis of blockage effects on urban cellular networks,” *IEEE Transactions on Wireless Communications*, vol. 13, no. 9, pp. 5070–5083, Sep. 2014.
[26] T. Bai and R. W. Heath, “Coverage and rate analysis for millimeter-wave cellular networks,” *IEEE Transactions on Wireless Communications*, vol. 14, no. 2, pp. 1100–1114, Feb. 2015.
[27] C. A. Balanis, *Antenna Theory: Analysis and Design*. Hoboken, NJ, USA: John Wiley & Sons, 2005.
[28] R. K. Ganti and M. Haenggi, “Asymptotics and approximation of the SIR distribution in general cellular networks,” *IEEE Transactions on Wireless Communications*, vol. 15, no. 3, pp. 2130–2143, Mar. 2016.
[29] M. Haenggi, *Stochastic geometry for wireless networks*. Cambridge University Press, 2012.
[30] A. Jeffrey and D. Zwillinger, *Table of integrals, series, and products*. Academic Press, 2007.
[31] M. Haenggi, “Outage, local throughput, and capacity of random wireless networks,” *IEEE Transactions on Wireless Communications*, vol. 8, no. 8, pp. 4350–4359, Aug. 2009.
[32] K. Feng and M. Haenggi, “A location-dependent base station cooperation scheme for cellular networks,” *IEEE Transactions on Communications*, vol. 67, no. 9, pp. 6415–6426, 2019.

Haichao Wei received the B.S. and Ph.D. degrees in information and communication engineering from the University of Science and Technology of China (USTC), Hefei, China, in 2010 and 2016, respectively. Currently he is a lecturer at Dalian Maritime University, Dalian, China. In 2016-2018 he was an Engineer at Huawei Technologies Co., Ltd., Shanghai, China. His research interests include heterogeneous and cellular networks, positioning technologies, stochastic geometry, green communications, and underwater acoustic communications.

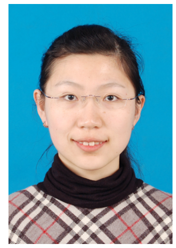

Na Deng (S’12-M’17) received the B.S. and Ph.D. degrees in information and communication engineering from the University of Science and Technology of China (USTC), Hefei, China, in 2010 and 2015, respectively. Currently she is an Associate Professor at Dalian University of Technology, Dalian, China. In 2013-2014, she was a Visiting Student in Prof. Martin Haenggi’s group at the University of Notre Dame, Notre Dame, IN, USA, and in 2015-2016 she was a Senior Engineer at Huawei Technologies Co., Ltd., Shanghai, China. Her scientific interests include networking and wireless communications, intelligent communications, and space-air-ground integrated networks.

Martin Haenggi (S’95-M’99-SM’04-F’14) received the Dipl.-Ing. (M.Sc.) and Dr.sc.techn. (Ph.D.) degrees in electrical engineering from the Swiss Federal Institute of Technology in Zurich (ETHZ) in 1995 and 1999, respectively. Currently he is the Freimann Professor of Electrical Engineering and a Concurrent Professor of Applied and Computational Mathematics and Statistics at the University of Notre Dame, Indiana, USA. In 2007-2008, he was a Visiting Professor at the University of California at San Diego, in 2014-2015 he was an Invited Professor at EPFL, Switzerland, and in 2021-2022 he is a Guest Professor at ETHZ. He is a co-author of the monographs “Interference in Large Wireless Networks” (NOW Publishers, 2009) and “Stochastic Geometry Analysis of Cellular Networks” (Cambridge University Press, 2018) and the author of the textbook “Stochastic Geometry for Wireless Networks” (Cambridge, 2012) and the blog stogblog.net, and he published 18 single-author journal articles. His scientific interests lie in networking and wireless communications, with an emphasis on cellular, amorphous, ad hoc (including D2D and M2M), cognitive, vehicular, and wirelessly powered networks. He served as an Associate Editor for the Elsevier Journal of Ad Hoc Networks, the IEEE Transactions on Mobile Computing (TMC), the ACM Transactions on Sensor Networks, as a Guest Editor for the IEEE Journal on Selected Areas in Communications, the IEEE Transactions on Vehicular Technology, and the EURASIP Journal on Wireless Communications and Networking, as a Steering Committee member of the TMC, and as the Chair of the Executive Editorial Committee of the IEEE Transactions on Wireless Communications (TWC). From 2017 to 2018, he was the Editor-in-Chief of the TWC. Currently he is an editor for MDPI Information. For both his M.Sc. and Ph.D. theses, he was awarded the ETH medal. He also received a CAREER award from the U.S. National Science Foundation in 2005 and three paper awards from the IEEE Communications Society, the 2010 Best Tutorial Paper award, the 2017 Stephen O. Rice Prize paper award, and the 2017 Best Survey paper award, and he is a Clarivate Analytics Highly Cited Researcher.